



THE UNIVERSITY *of* EDINBURGH

## Edinburgh Research Explorer

# Interaction of Inherent Minerals with Carbon during Biomass Pyrolysis Weakens Biochar Carbon Sequestration Potential

### Citation for published version:

Nan, H, Yang, F, Zhao, L, Masek, O, Cao, X & Xiao, Z 2018, 'Interaction of Inherent Minerals with Carbon during Biomass Pyrolysis Weakens Biochar Carbon Sequestration Potential', *ACS Sustainable Chemistry & Engineering*. <https://doi.org/10.1021/acssuschemeng.8b05364>

### Digital Object Identifier (DOI):

[10.1021/acssuschemeng.8b05364](https://doi.org/10.1021/acssuschemeng.8b05364)

### Link:

[Link to publication record in Edinburgh Research Explorer](#)

### Document Version:

Peer reviewed version

### Published In:

ACS Sustainable Chemistry & Engineering

### Publisher Rights Statement:

© 2018 American Chemical Society

### General rights

Copyright for the publications made accessible via the Edinburgh Research Explorer is retained by the author(s) and / or other copyright owners and it is a condition of accessing these publications that users recognise and abide by the legal requirements associated with these rights.

### Take down policy

The University of Edinburgh has made every reasonable effort to ensure that Edinburgh Research Explorer content complies with UK legislation. If you believe that the public display of this file breaches copyright please contact [openaccess@ed.ac.uk](mailto:openaccess@ed.ac.uk) providing details, and we will remove access to the work immediately and investigate your claim.



**Contact information for all authors:**

Hong-Yan Nan  
School of Environmental Science and Engineering  
Shanghai Jiao Tong University  
Minhang, Shanghai 200240, China  
Tel: 86 21 54743926  
Fax: 86 21 54740825  
E-mail: [nanhongyan@sjtu.edu.cn](mailto:nanhongyan@sjtu.edu.cn)

Fan Yang  
School of Environment and Architecture  
University of Shanghai for Science and Technology  
Yangpu, Shanghai 200093, China  
Tel: 86 21 54743926  
Fax: 86 21 54740825  
E-mail: [yangfanusst@usst.edu.cn](mailto:yangfanusst@usst.edu.cn)

Ling Zhao\*  
School of Environmental Science and Engineering  
Shanghai Jiao Tong University  
Minhang, Shanghai 200240, China  
Tel: 86 21 54743926  
Fax: 86 21 54740825  
E-mail: [wszhaoling@sjtu.edu.cn](mailto:wszhaoling@sjtu.edu.cn)

Ondřej Mašek  
School of Geosciences,  
University of Edinburgh  
Kings Buildings, Edinburgh, EH9 3JN, UK  
Tel: 0131 6505095  
Fax: +44 131 662 0478  
E-mail: [ondrej.masek@ed.ac.uk](mailto:ondrej.masek@ed.ac.uk)

Xin-De Cao  
School of Environmental Science and Engineering  
Shanghai Jiao Tong University  
Minhang, Shanghai 200240, China  
Tel: 86 21 34202841  
Fax: 86 21 54740825  
E-mail: [xdcao@sjtu.edu.cn](mailto:xdcao@sjtu.edu.cn)

Zi-Yue Xiao  
School of Environmental Science and Engineering  
Shanghai Jiao Tong University  
Minhang, Shanghai 200240, China  
Tel: 86 21 54743926  
Fax: 86 21 54740825  
E-mail: [KiseRyota@sjtu.edu.cn](mailto:KiseRyota@sjtu.edu.cn)

# **Interaction of Inherent Minerals with Carbon during Biomass Pyrolysis Weakens Biochar Carbon Sequestration Potential**

Hongyan Nan,<sup>†</sup> Fan Yang,<sup>‡</sup> Ling Zhao,<sup>†,\*</sup> Ondřej Mašek,<sup>§</sup> Xinde Cao,<sup>†</sup> and Ziyue Xiao<sup>†</sup>

<sup>†</sup>School of Environmental Science and Engineering, Shanghai Jiao Tong University, Shanghai  
200240, China

<sup>‡</sup>School of Environment and Architecture, University of Shanghai for Science and  
Technology, Shanghai 200093, China

<sup>§</sup> School of Geosciences, University of Edinburgh, Kings Buildings, Edinburgh, EH93JN, UK

\*Corresponding authors:

Tel: +86-21-54743926; Fax: +86-21-54740825; e-mail: [wszhaoling@sjtu.edu.cn](mailto:wszhaoling@sjtu.edu.cn) (Ling Zhao)

## ABSTRACT

Biomass carbon could be sequestered in form of biochar, an aromatized carbon structure produced by pyrolysis. Inherent minerals are reactive constituents that interact with organic contents during pyrolysis, significantly affecting the properties of the pyrolysis product. Despite their importance, their influence on biochar-carbon sequestration has been rarely studied. This study selected four types of biomass: barley grass, peanut hull, cow manure and sewage sludge to investigate the influence of inherent minerals on carbon conversion during pyrolysis. Results showed removal of inherent minerals shifts the peak biomass conversion to a higher temperature (370°C) compared to biomass with inherent minerals being present (330°C). It also led to reduced emissions of low molecular weight organic compounds. Compared to pristine biomass, more carbon (3.5-30.1%) could be retained in biochar along pyrolysis after removing inherent minerals. And it showed increased resistance to chemical and thermal oxidation decomposition, indicating higher carbon stability and therefore carbon sequestration potential. Instrumental analysis showed removal of inherent minerals facilitated disappearance of oxygen-containing functional groups such as C=O, O=C-O and C-O, while promoting C-C/C=C bonds, indicating higher aromatization of biochars. This study suggested that to remove minerals prior to pyrolysis can be a promising approach for strengthening carbon-sequestration potential of biochar.

**KEYWORDS:** *Biochar, Inherent minerals, Carbon retention, Oxidation resistance, Chemical state of carbon*

## INTRODUCTION

The issue of climate change and global warming has been gaining increasing attention in recent years, including technologies for managing greenhouse gases (GHG) emissions into atmosphere.<sup>1,2</sup> Besides techniques focused on removal of GHG (mainly CO<sub>2</sub>) emissions from large point sources, technologies for removal of carbon indirectly from the atmosphere have also been proposed and intensively researched. Humanity appropriates net primary biomass production, and this generates a large volume of waste biomass, including plant and animal residues.<sup>3</sup> The carbon contained in these organic residues is usually released into the atmosphere through natural processes (biodegradation) or human activities (e.g., incineration), and therefore presents an important source of GHG contributing the major source of GHG.<sup>4</sup> Biochar, as a pyrolytic carbonization material, comes from the waste biomass under the condition of limited O<sub>2</sub> and a relatively low temperature (300-700°C). It is a promising strategy of carbon sequestration, which has been widely studied in the past decade.<sup>5,6</sup> Previous work has demonstrated that biochar could be stored in soil as a stable carbon pool.<sup>7,8</sup> The ability of biochar to sequester carbon depends on the carbon retention ratio in solid product after pyrolysis, the oxidation/degradation resistance of biochar,<sup>9-12</sup> and the interaction of biochar with soil components, etc.<sup>13</sup> All these factors are highly related to the microstructure and chemical composition of the biochar, which is in turn dependent on biomass feedstock and pyrolysis conditions.<sup>3</sup>

Inherent minerals in various biomasses, including various metal elements (K, Na, Ca, Mg, Fe, etc.), are a significant component with considerable impacts on its properties and performance in thermochemical conversion.<sup>3</sup> Despite an extensive body of published research on biochar carbon stability, no systematic investigation of the effects of inherent minerals on carbon sequestration potential of biochar has been reported to date.<sup>14</sup> In fact, inherent biomass minerals are quite reactive and have a potential catalytic effect during pyrolysis.<sup>15,16</sup> It was found that the inorganic minerals could alter the distribution of the solid, liquid, and gaseous products during the pyrolysis process.<sup>17</sup> They could even make more homogeneous

constituents with relatively small molecules.<sup>18, 19</sup> For instance, Patwardhan et al.<sup>20</sup> and Shimada et al.<sup>21</sup> demonstrated that inorganic salts ( $K^+$ ,  $Na^+$ ,  $Ca^{2+}$ ,  $Mg^{2+}$ ) increased the gaseous yield of low molecular species. Liu et al.<sup>22</sup> reported that Cu promoted bio-oil formation during pyrolysis of the wood chips. This was ascribed to the ability of Cu to catalyze lignin degradation into smaller molecules. Other studies showed opposite effects. Kinata et al.<sup>23</sup> found that wood chips containing  $KCr(SO_4)_2$  and  $H_3BO_3$  yielded less CO and  $CO_2$ , but more charcoal in their pyrolysis products. Previous findings mainly focused on pyrolysis products concerning energy recycling, while few studies paid attention to how inherent minerals influence the microstructure of carbon and the implications to carbon sequestration.

In this study, we conducted a series of experiment to 1) investigate how inherent minerals in biomass influence their thermal decomposition and carbon sequestration capacity of biochar; 2) detect the surface functional groups and chemical state of C on biochar, as well as the microstructure of biochar-carbon for elucidating the effect of minerals on carbon evolution during biochar formation; 3) explore the minerals-carbon interactions via detecting the carbon evolution under a series of pyrolysis temperatures.

## MATERIALS AND METHODS

**Removal of Inherent Minerals from Biomass.** Four types of common biomass, barley grass (BG), peanut hull (PH), cow manure (CM), and sewage sludge (SS) representing a range of agricultural and municipal organic residues with different inherent mineral constituents were collected from Shanghai, China. Biomass was air-dried and shredded into approx. 1 cm particles (XL-6B, China), and further was sieved through 2 mm sieve. According to the different biomass shapes and properties, the particle size distribution of barley grass and peanut hull ranged from 1 mm to 2 mm, and that of dairy manure and sewage sludge ranged from 0.5 mm to 2 mm. To remove inherent minerals, a mixture of  $0.5 \text{ mol} \cdot \text{L}^{-1}$  HCl and  $0.5 \text{ mol} \cdot \text{L}^{-1}$  HF was used to rinse the biomass ( $w/v=1/30$ ).<sup>24</sup> The biomass and acid solution were mixed evenly and shocked for 24 h. After acid treatment, the biomasses were washed to a neutral pH with deionized water by filter gauze, and then they were placed in oven under

80°C for 24 h-drying. After removing minerals, the particle size distribution of barley grass and peanut hull showed little change, and still maintained between 1mm and 2mm. While the particle size distribution of dairy manure and sewage sludge increased from 0.5-2 mm to 1-2 mm due to the slight aggregation. This process removed almost all inherent minerals and minute quantities of dissolved carbon (disregarded). Table 1 showed the inherent minerals removal rates of four biomasses by the change of the ash contents before and after acid treatment. And there were less impact on the followed calculation about carbon retention and stability. For simplicity, the demineralized barley grass, peanut hull, cow manure, and sewage sludge were named as DM-BG, DM-PH, DM-CM, and DM-SS. Their elemental compositions are shown in [Table 1](#).

**Biochar Production and Characterization.** Biochars were produced in a tube furnace pyrolysis system under N<sub>2</sub> atmosphere. Pyrolysis process was performed at a heating rate of 15°C·min<sup>-1</sup>, and the samples were held for 2 h at the final temperature of 500°C. This temperature was selected considering the balance of carbonization degree and the yield and cost. Then the samples were cooled down under oxygen-limited conditions. The samples were grinded to fine powder in a ball mill (QM-3SPO4, China) and stored in a dryer for analyses. Biochar pH was measured after shaken for 10 min in distilled water using a digital pH meter (pH510, alalis, USA) with a solid-to-liquid ratio of 1:20 (w/v).<sup>25</sup> Content of C, H, N and S in biochar was analyzed using an elemental analyzer (Vario EL III, Elementar, Germany). Ash content of biochar was determined by weight loss after heating to 550°C in an oxygen atmosphere for 4 h. <sup>3</sup> Crystalline structure of biochar was evaluated by X-ray diffractometer (XRD, D/max-2200/PC, Rigaku, Japan) with a scan speed of 2°·min<sup>-1</sup> and scan angle ranging from 10° to 80°. All the measured biochar properties are shown in [Table S1](#) and [Figure S1](#).

**Biomass Decomposition and Carbon Retention in Biochar.** The conversion rate of organic matter was calculated based on the difference of organic fraction before and after the pyrolysis. The carbon retention was calculated by contrasting the carbon contents of biochar and biomass. The experiment was run in triplicate.

$$\text{Organic matter conversion (\%)} = \frac{W_{\text{biochar}} - W_{\text{minerals}}}{W_{\text{biomass}} - W_{\text{minerals}}} \times 100\% \quad (1)$$

$$\text{Carbon retention (\%)} = \frac{C_{\text{biochar}}}{C_{\text{biomass}}} \times Y_{\text{biochar}} \quad (2)$$

Where  $W_{\text{biochar}}$  and  $W_{\text{biomass}}$  are the weight (%) of biochars and biomass, respectively, while  $W_{\text{minerals}}$  is the minerals weight (%), i.e., ash content. The  $C_{\text{biochar}}$  and  $C_{\text{biomass}}$  are carbon contents (%) of the biochar and biomass, respectively, and  $Y_{\text{biochar}}$  is the yield (%) of biochar. In order to research the dynamical pyrolysis process, a thermogravimetric-mass spectrometry (TGA/DSC1, Netzsch, Germany) was used to emulate the biochar production conditions experienced by the biomass under  $N_2$  atmosphere ( $300 \text{ mL} \cdot \text{min}^{-1}$ ) in tube furnace system. The mass loss of biomass and the gas release were monitored simultaneously.

**Oxidation Resistance and Carbon Microstructure of Biochar.** The surface functional groups were detected by FTIR spectroscopy (IR Prestige 21 FTIR, Shimadzu, Japan). The long-term stability could be assessed via chemical  $K_2Cr_2O_7$  oxidation and TGA in air/ $O_2$ ,<sup>13,26</sup> since these could simulate the disintegration of carbon skeleton in a simulative extreme oxidation environment.<sup>27</sup> More details could be found in the Supporting Information. The Raman Spectroscopy (Senterra R200-L, Bruker Optics, Germany) were used for analyzing the carbon microstructure of biochar.

**Interaction of Inherent Minerals and Carbon in Pyrolysis Process.** To elucidate the interaction of inherent minerals and carbon during biomass pyrolysis, one biomass type (cow manure) was selected to produce biochar in a series of temperature ( $300^\circ\text{C}$ ,  $400^\circ\text{C}$ ,  $500^\circ\text{C}$ , and  $600^\circ\text{C}$ ) and several instrumental analyses were conducted. Cow manure was selected because it contained more common minerals such as K, Ca, Mg, etc, compared with other biomass. X-ray photoelectron spectroscopy (XPS, AXIS Ultra DLD, Shimadzu Kratos, Japan) was performed to detect the bonding energy of carbon on biochar surface. The constituents of the pyrolyzed gas were online using a thermogravimetric analyzer connected to an FTIR spectrometer and gas chromatography mass spectrometer (TG-FTIR-GCMS, TGI/GCMS/TGA8000, USA).



## RESULTS AND DISCUSSION

**Inherent Minerals Reduced the Carbon Retention of Biochar.** There was a large distinction of the inherent minerals contents among these four types of biomass ([Table 1](#)). As expected, K, Ca, Mg, Fe, Al were the main components in these biomass residues. Acid washing significantly removed these minerals with their contents being reduced by 88.7%, 81.7%, 85.3% and 51.5% for barley grass, peanut hull, cow manure and sewage sludge, respectively. The low ash removal rate of sewage sludge (51.5%) indicated the presence of insoluble inorganic sediments. As shown in [Figure S1](#), in plant residues, KCl, calcite ( $\text{CaCO}_3$ ), whitlockite ( $(\text{Ca, Mg})_3(\text{PO}_4)_2$ ), and calcium oxalate ( $\text{Ca}(\text{COO})_2$ ) were detected, while in sewage sludge, the main species of Fe and Al were hydroxyl oxidize iron ( $\text{FeOOH}$ ) or aluminum hydroxide ( $\text{Al}(\text{OH})_3$ ). Detailed profile of inherent minerals in biomass is presented in [Table 1](#).

The demineralization decreased the yield of biochar from 27.8-48.0% (dry basis) to 24.9-43.0% (dry basis), but raised the carbon content from 21.9-69.8% to 36.6-81.8% (ash free basis) ([Table S1](#)). With minerals removal, the conversion rate of the organic matter was raised by 15.3%, 5.60%, 16.6% and 61.6% for BG, PH, CM, and SS, respectively. Accordingly, the carbon retained in biochar after pyrolysis were raised by 3.66%, 2.76%, 6.68% and 23.1%, respectively ([Figure 1](#)). Compared to CM and SS, the contents of inherent minerals in BG and PH were much lower ([Table 1](#)), suggesting that removal of inherent minerals seemed to have positive effect on carbon retention.

### **Inherent Minerals Intensified Decomposition of Carbon during Biomass Pyrolysis.**

The results of TGA and DTG ([Figure 2](#)) confirmed that the inherent minerals intensified the decomposition of carbon in biomass during the pyrolysis. There are two peaks on the DTG curves for almost all the biomasses. For the pristine biomasses, the first peak appeared at about 300°C, and the second peak appeared at about 330°C while for the demineralized biomasses, the second peak moved to 370°C. Also, the intensity of the second peak of the demineralized biomass was much higher than that of the pristine biomass, except for the

sewage sludge. This means that removal of minerals (K, Ca, Mg) greatly promoted the biomass decomposition corresponding to the second peak, however this occurred at a higher temperature compared to the raw biomass. This phenomenon was attributed to the catalytic effect of inherent minerals on thermal conversion of key biomass constituents, such as, lignin, cellulose and hemicellulose.<sup>28, 29, 30</sup> Significant influence of minerals on biomass decomposition typically appears at 300-400°C, since the cellulose and lignin decompose in this temperature range. This leads to a transformation of the carbon skeleton into amorphous state with generating a lot of small molecule organic compounds such as CO<sub>2</sub>, CH<sub>4</sub>, C<sub>2</sub>H<sub>4</sub>O<sub>2</sub>, etc.<sup>22, 31</sup>

The release of the small molecular substances also proved that inherent minerals could catalyze degradation of carbon structure (Figure S2). It was obvious that the peaks of CO<sub>2</sub>, CH<sub>4</sub>, C<sub>2</sub>H<sub>4</sub>O<sub>2</sub>, C<sub>3</sub>H<sub>6</sub>O, C<sub>3</sub>H<sub>6</sub>O<sub>2</sub>, and C<sub>4</sub>H<sub>4</sub>O of the pristine biomasses were much higher than those of the demineralized biomasses, except for the sewage sludge. The integral area of these peaks were listed in Table S2. Alkali and alkaline earth metal played an important role in catalyzing the decomposition of biomass.<sup>32</sup> K-containing compounds catalyzed the secondary cracking of volatiles produced in the pyrolysis process to generate more small gas compounds (e.g., CO, H<sub>2</sub>, CH<sub>4</sub>, C<sub>2</sub>H<sub>4</sub>, CO<sub>2</sub>).<sup>33</sup> Ca-containing compounds could control the cleavage of the glycosidic bonds in cellulose impacting yields of levoglucosan and cellobiosan.<sup>34</sup> In our study, this phenomenon was particularly obvious for the plant-like biomasses containing more K, Ca, and Mg. In contrast, sewage sludge contained more Fe and Al, which potentially made it draw an opposite conclusion. Previous research suggested that Fe<sub>2</sub>O<sub>3</sub> and activated Al<sub>2</sub>O<sub>3</sub> hindered the earlier degradation of volatile components such as fat and protein.<sup>35</sup> Thus the demineralization of sludge caused the peak decomposition appeared at a lower temperature.

**Inherent Minerals Weakened the Oxidation Resistance of Biochar-Carbon.** The carbon sequestration capacity of biochar depends on its stability in environment, which could be evaluated by the oxidation resistance of biochar-carbon. The chemical state of C on biochar surface and C loss in oxidizing agent were detected to offer information about short-term and

long-term stability of biochar-carbon.

Surface functional groups carrying biochar-carbon played an important role in the oxidation resistance of biochar-carbon.<sup>36</sup> The presence or absence of minerals presented a deviation in some of peaks for these formed functional groups ([Figure 3](#)). Ablation of hydroxyl (-OH) and aliphatic CH<sub>2</sub> during pyrolysis seemed less influenced by minerals, which was represented by peaks at 3404 cm<sup>-1</sup> and 2909 cm<sup>-1</sup>.<sup>36</sup> Peaks at 1575 cm<sup>-1</sup>, representing aromatic C=C/C=O, were higher in the demineralized biochars than the original ones,<sup>31</sup> especially in the cow manure biochar, which had a highest amount of minerals removal ([Table 1](#)).<sup>31,37,38</sup> Whereas this change was not obvious in sewage sludge biochar. A significant difference at peaks of 1405-1041 cm<sup>-1</sup> was observed before and after the removal of inherent minerals indicating that the absence of inherent minerals facilitated the disappearance of -CH<sub>2</sub>, C-O and C-O-C.<sup>37, 39</sup> Perhaps inherent minerals hindered the aromatization process via retaining more O-containing functional groups such as phenolic monomers or via hindering their release.<sup>39</sup> Stretching vibration of Si-O-Si groups (1041 cm<sup>-1</sup> and 800 cm<sup>-1</sup>)<sup>37, 41, 42</sup> were widespread in all the biochars, which seemed not affected by demineralization, which accorded with the obvious diffraction peak of SiO<sub>2</sub> in the XRD curves ([Figure S1](#)). These results infer that inherent minerals perhaps have a negative effect on the formation of aromatic carbon.

To further understand the chemical state of C on the biochar surface, the cow manure biochar with the most abundant minerals was selected to analyze the bond energy of C 1s using X-ray photoelectron spectroscopy (XPS) ([Figure S3](#)). The energy spectrum consisted of five peaks including C-C/C=C at 284-285 eV, alcoholic hydroxyl, phenolic hydroxyl or ether C-O at 285.4-286.0 eV, carbonyl or quinonyl C=O at 287 eV,<sup>43-45</sup> and carboxyl or ester O=C-O at 288.2-288.7 eV.<sup>46, 47</sup> The percent of C-containing surface groups was listed in [Table 2](#). The C=O and O=C-O only appeared in the original biochar. Furthermore, the percent of C-O was triple in the original biochar than that in the demineralized biochar. Oppositely, the content of C-C/C=C in the demineralized biochar was obviously higher than that in the

original biochar. These results accorded with the above results (Figure 3) greatly, gathering our focus on the O-containing functional groups. The conclusion could be confirmed that inherent minerals intensified thermal decomposition of carbon structure, while hindered the carbonization process, then weakened the oxidation resistance of biochar.<sup>48</sup>

The oxidation resistance of the whole carbon skeleton of biochar was determined by  $K_2Cr_2O_7$  oxidation, a simulated extreme oxidation environment.<sup>13</sup> The oxidized carbon by  $K_2Cr_2O_7$  was assumed as the unstable fraction of the biochar-carbon. It could be seen from Figure 4 that inherent minerals promoted more carbon to transform into unstable carbon in the pyrolysis process. The calculation basing on the dry basis of biomass showed that the mineral removal not only reduced the total carbon loss, but also increased the stable fraction of the biochar-carbon by 27.7-75.4%. It was noted that although demineralized sewage sludge still contained a considerable content of Fe (0.558%) and Al (0.243%) (Table 1), it also had a relatively high stable fraction of biochar-carbon, indicating that Fe and Al were not the catalyst that promoted carbon to transform into unstable carbon.<sup>13</sup> The higher stability of the demineralized biochar was further demonstrated by their incineration curves in air (Figure S4). Yang et al.<sup>49</sup> also reported that de-ashing treatment increased the activation energy of all biochar samples, probably due to the changes of the chemical composition and conformation of carbon structure.

#### **Inherent Minerals tended to Drive Formation of Disordered Structure in Biochar.**

Raman spectra were obtained to analyze the microstructure of biochar.<sup>50</sup> Two clear peaks could be detected (Figure S5), one was corresponding to the in-plane vibrations of  $sp^2$ -bonded amorphous carbon structures with structural defects (D band at  $1350\text{ cm}^{-1}$ ), and the other was corresponding to the in-plane vibrations of the  $sp^2$ -bonded graphitic carbon structures (G band at  $1575\text{ cm}^{-1}$ ).<sup>51</sup> The  $I_D/I_G$  correlated negatively to the graphitization degree of carbon structure. Fitting curves of the bands were integrated to calculate the area, being  $I_D$ ,  $I_G$  and  $I_{All}$ . When minerals were removed from the plant-like biomass,  $I_D/I_G$  of the biochars decreased, while  $I_G/I_{All}$  increased (Table 3). Specifically,  $I_D/I_G$  of the BG-biochar, PH-biochar, CM-

biochar decreased from 1.23 to 1.07, 1.18 to 1.11, 1.34 to 1.13, respectively, while SS-biochar was increasing from 1.16 to 1.22. Thus inherent minerals tended to drive formation of disordered structure or structural defects in biochar, which decreased the aromaticity of their carbon structure.<sup>48, 52</sup>

**How Inherent Minerals Interacted with Biomass-Carbon along Pyrolysis?** Based on the above results, removing inherent minerals posed an obvious influence on carbon evolution during pyrolysis. It is worth noting that the influence of minerals on carbon retention increased along the rising pyrolysis temperature (Figure 5a).<sup>31, 53</sup> The oxidation resistance of biochar was also enhanced accordingly (Figure 5b). The dynamic thermal-chemical reactions could be analyzed from the results of TG-FTIR-GCMS (Table S3, Figure 6). The main gas products of cow manure pyrolysis including small molecules such as Acetic acid, Chloromethane, Acetaldehyde, Butane, etc., and middle molecular substances mainly being Furfural, Pyrazole, or Furan, as well as some large molecular weight matters, D-glucopyranoside, Cyclopropanecarbonyl chloride, Cortisol, Cholestane, etc. As can be seen from Table S3, both the original and the demineralized biomass showed a first peak decomposition temperature at 300°C, while their second decomposition peak occurred at 330°C and 370°C, respectively. At 300°C, the pristine biomass with the existence of inherent minerals produced a relatively high percent of small molecules (48.8%) in the pyrolytic bio-gas, while this value was as low as only 0.937% for the demineralized treatment, simultaneously the middle molecular (0.844%) and large molecular substances (5.87%) were detected. At the second peak, they both generated a similar percent of large molecular weight matter (8-10%). The pristine biomass still released a fraction of small molecular substances (1.22%), while the demineralized one generated a little middle molecular substances (0.418%) (Table S3).

Significant influences of inherent minerals on the functional groups of gaseous pyrolysis product appeared mainly from the first decomposition peak (Figure 6). More O-containing substances (wavenumber around 1000 cm<sup>-1</sup>) released as large molecular substances for the

demineralized cow manure (Figure 6b), compared to the original cow manure (Figure 6a).

This was consistent with the result that less O-containing functional groups retained on the demineralized biochar surface. The influence of minerals lasted to the end of the pyrolysis, resulting in more release of carbon as aromatized molecules (Figure 6a).

Before pyrolysis, minerals are inlaid in the plant tissues, then they are emitted during the temperature of 250-400°C, and can be further released from the ash fraction at temperatures higher than 600°C.<sup>54</sup> Kowalski et al.<sup>55</sup> monitored alkali metal and alkaline-earth metals release and found that one peak of metal emission was in 300-400°C, while the other peak is at temperatures higher than 600°C. The first one is attributed to the decomposition of organic metal salts, while the second one is due to the evaporation of inorganic metal compounds. Reactions were assumed occurring in aerosols produced directly from the pyrolysis of biomass particles or through the superheated volatiles ejected out of biomass particle pores, which were made of submicrometer liquid droplets. The fine biochar particles entrained out from the separation system may serve as condensation nuclei for the aerosols containing alkali metal species. In this atmosphere, R-O-K, RCOO-K were formed via decomposition of organic K and the evaporated KCl (gas). Aromatization forwards along charring with rising pyrolysis temperature and R-aromatic-O-K was formed under pyrolysis temperature of 600°C.<sup>54</sup>

The catalytic effects of alkali metal minerals have been proved in many previous studies. Inorganic salts as low as 0.005 mmols·g<sup>-1</sup> of cellulose were found sufficient to dramatically change the primary reactions that led to the formation of lower molecular weight species (especially formic acid, glycolaldehyde and acetol).<sup>20</sup> As a result of faster competing reactions, lower levoglucosan yields were observed, which was a key intermediate substance would undergo dehydration, C-O bond scission, and C-C bond scission to form the aromatic carbon.<sup>54</sup> Hu et al.<sup>56</sup> elucidated that inherent alkali metals could enhance water-gas shift reaction and accelerated significantly the decomposition of levoglucosan, and meanwhile also could promote breakage and restructuring of hetero atoms.

As the indispensable constituent of biomass, the small amounts of metallic minerals in biomass play an important catalytic role in controlling the carbon sequestration capacity in pyrolysis process. Previous findings mainly focused on pyrolysis products concerning energy recycling, while few studies paid attention to how inherent minerals influence the microstructure of carbon, and the implications to carbon sequestration. In this study, the interaction between biomass-carbon and biomass-minerals along pyrolysis and the influences on carbon sequestration were explored, presenting a distinct insight to enhance the carbon sequestration efficiency. It should be noted that the effect of each type of inherent minerals to biochar-carbon sequestration along pyrolysis should be singly investigated in the future study.

## CONCLUSION

Inherent biomass minerals are reactive constituents that interact with organic constituents during pyrolysis, significantly affecting the product distribution and properties. This study showed that inherent minerals, K, Ca, and Mg rather than Fe and Al could intensify thermal decomposition of carbon skeleton, making the bulk weight loss occur in a lower temperature (330°C), compared to that without minerals (370°C). Thus more carbon emitted with gas as low molecular weight organic matters (CO<sub>2</sub>, CH<sub>4</sub>, C<sub>3</sub>H<sub>6</sub>O, etc.) resulting to a reduction of carbon retention in biochar by 3.5-30.1%. Moreover, inherent minerals weakened oxidation resistance of biochar-carbon, with a significant reduction of stable carbon by 27.7-75.4% after K<sub>2</sub>Cr<sub>2</sub>O<sub>7</sub> oxidation. Instrumental analysis (FTIR, Raman spectrum, TG-FTIR-MS, XPS) showed that presence of minerals induced more formation of oxygen containing functional group such as C=O, O=C-O, C-O-C and C-O. Removing minerals facilitated disappear of them, and increased C-C/C=C as aromatization of biochars were strengthened. It was assumed that R-O-K, RCOO-K were formed via evaporated KCl (gas). Inherent minerals tended to drive formation of disordered structure indicated by decreased I<sub>D</sub>/I<sub>G</sub> of all biochars when minerals were removed. This study offered a new sight for strengthening biochar carbon sequestration potential.

## **AUTHOR INFORMATION**

### **Corresponding Author**

\*Telephone: +86-21-54743926. Fax: +86-21-54740825. E-mail:

wszhaoling@sjtu.edu.cn.

### **Notes**

The authors declare no competing financial interests.

## **ACKNOWLEDGMENTS**

This work was supported in part by the National Natural Science Foundation of China (Project No. NSFC 21577087, NSFC key project 21537002), and by the National water pollution control key project (2017ZX07204002-03, 2017ZX07202005-005).

## **ASSOCIATED CONTENT**

### **Supporting Information**

Profile of inherent minerals in different types of biomass. The stability measurement:  $K_2Cr_2O_7$  oxidation method. Table S1 Selected physical and chemical properties of the biochar. Table S2 Relative amount of low molecular weight organic matters in the pyrolysis gas. Table S3 Main chemical substances generated from cow manure pyrolysis at the bulking weight loss temperature. Figure S1 XRD patterns of the biochars. Figure S2 Release of small organic molecules during biomass pyrolysis detected by TG-MS. Figure S3 XPS analysis of the biochars derived from the original cow manure (CM) and the demineralized cow manure (DM-CM). Figure S4 TGA and DTG curves of the biochars under  $O_2$  atmosphere to evaluate their thermal stability. Figure S5 Raman spectra of the biochars. Figure S6 Organic carbon loss rate of the biochars after  $K_2Cr_2O_7$  chemical oxidation. Figure S7 FTIR spectra of the biochars derived from the original cow manure (CM) and the demineralized cow manure



(DM-CM) at pyrolysis temperature of 300-600°C.

## REFERENCE

- (1) Mukherjee, A.; Zimmerman, A. R.; Harris, W. Surface chemistry variations among a series of laboratory-produced biochars. *Geoderma* **2011**, *163*, 247-255.
- (2) Cantrell, K. B.; Hunt, P. G.; Uchimiya, M.; Novak, J. M.; Ro, K. S. Impact of pyrolysis temperature and manure source on physicochemical characteristics of biochar. *Bioresour. Technol.* **2012**, *107*, 419.
- (3) Zhao, L.; Cao, X.; Wang, Q.; Yang, F.; Xu, S. Mineral constituents profile of biochar derived from diversified waste biomasses: implications for agricultural applications. *J. Environ. Qual.* **2013**, *42*, 545.
- (4) Dresbøll, D. B.; Magid, J. Structural changes of plant residues during decomposition in a compost environment. *Bioresour. Technol.* **2006**, *97*, 973.
- (5) Meyer, S.; Bright, R. M.; Fischer, D.; Schulz, H.; Glaser, B. Albedo impact on the suitability of biochar systems to mitigate global warming. *Environ. Sci. Technol.* **2012**, *46*, 12726.
- (6) Whitman, T.; Nicholson, C. F.; Torres, D.; Lehmann, J. Climate change impact of biochar cook stoves in western Kenyan farm households: system dynamics model analysis. *Environ. Sci. Technol.* **2011**, *45*, 3687.
- (7) Zhao, L.; Cao, X.; Mašek, O.; Zimmerman, A. Heterogeneity of biochar properties as a function of feedstock sources and production temperatures. *J. Hazard. Mater.* **2013**, *s 256–257*, 1-9.
- (8) Meyer, S.; Glaser, B.; Quicker, P. Technical, economical, and climate-related aspects of biochar production technologies: a literature review. *Environ. Sci. Technol.* **2011**, *45*, 9473.
- (9) Cross, A.; Sohi, S. P. A method for screening the relative long-term stability of biochar. *GCB. Biology* **2013**, *5*, 215–220.
- (10) Cornelissen, G.; Rutherford, D. W.; Arp, H. P.; Dörsch, P.; Kelly, C. N.; Rostad, C. E. Sorption of pure N<sub>2</sub>O to biochars and other organic and inorganic materials under anhydrous conditions. *Environ. Sci. Technol.* **2013**, *47*, 7704.
- (11) Zimmerman, A. R. Abiotic and microbial oxidation of laboratory-produced black carbon (biochar). *Environ. Sci. Technol.* **2010**, *44*, 1295-1301.
- (12) Keith, A.; Singh, B.; Singh, B. P. Interactive priming of biochar and labile organic matter mineralization in a smectite-rich soil. *Environ. Sci. Technol.* **2011**, *45*, 9611-9618.
- (13) Fan, Y.; Ling, Z.; Gao, B.; Xu, X.; Cao, X. The Interfacial Behavior between Biochar and Soil Minerals and Its Effect on Biochar Stability. *Environ. Sci. Technol.* **2016**, *50*, 2264-2271.
- (14) Xu, X.; Zhao, Y.; Sima, J.; Zhao, L.; Mašek, O.; Cao, X. Indispensable role of biochar-inherent mineral constituents in its environmental applications: A review. *Bioresour. Technol.* **2017**, *241*, 887-899.
- (15) Martinez, A. Mineral Matter Characterization in Olive Stones by Joint Use of LTA, XRD, FT-IR and SEM-EDX. *Appl. Spectrosc.* **2000**, *54*, 1712-1715.
- (16) Ross, A. B.; Anastasakis, K.; Kubacki, M.; Jones, J. M.; Gonzalezperez, J. A.; Gonzalezvila, F. J.; Rodriguezrodriguez, A. Investigation of the pyrolysis behaviour of brown algae before and after pre-treatment using PY-GC/MS and TGA. *J. Anal. Appl. Pyrolysis* **2009**, *85*, 3-10.
- (17) Yang, H.; Yan, R.; Chen, H.; Zheng, C.; Dong, H. L.; Liang, D. T. Influence of mineral matter on pyrolysis of palm oil wastes. *Combust. Flame* **2006**, *146*, 605-611.
- (18) Zhang, H.; Xiao, R.; Jin, B.; Xiao, G.; Chen, R. Biomass catalytic pyrolysis to produce olefins and aromatics with a physically mixed catalyst. *Bioresour. Technol.* **2013**, *140*, 256.
- (19) Shang, H.; Lu, R. R.; Shang, L.; Zhang, W. H. Effect of additives on the microwave-assisted

- pyrolysis of sawdust. *Fuel Process. Technol.* **2015**, *131*, 167-174.
- (20) Patwardhan, P.; Satrio, J.; Brown, R.; Shanks, B. Influence of inorganic salts on the primary pyrolysis products of cellulose. *Bioresour. Technol.* **2010**, *101*, 4646-4655.
- (21) Shimada, N.; Kawamoto, H.; Saka, S. Different action of alkali/alkaline earth metal chlorides on cellulose pyrolysis. *J. Anal. Appl. Pyrolysis* **2008**, *81*, 80-87.
- (22) Liu, W. J.; Tian, K.; Jiang, H.; Zhang, X. S.; Ding, H. S.; Yu, H. Q. Selectively improving the bio-oil quality by catalytic fast pyrolysis of heavy-metal-polluted biomass: take copper (Cu) as an example. *Environ. Sci. Technol.* **2012**, *46*, 7849.
- (23) Kinata, S. E.; Loubar, K.; Bouslamti, A.; Belloncle, C.; Tazerout, M. Influence of impregnation method on metal retention of CCB-treated wood in slow pyrolysis process. *J. Hazard. Mater.* **2012**, *s* 233-234, 172-176.
- (24) Das, P.; Ganesh, A.; Wangikar, P. Influence of pretreatment for deashing of sugarcane bagasse on pyrolysis products. *Biomass Bioenergy* **2004**, *27*, 445-457.
- (25) Zhao, L.; Cao, X.; Zheng, W.; Scott, J. W.; Sharma, B. K.; Chen, X. Copyrolysis of Biomass with Phosphate Fertilizers To Improve Biochar Carbon Retention, Slow Nutrient Release, and Stabilize Heavy Metals in Soil. *ACS Sustainable Chem. Eng.* **2016**, *21*, 409-414.
- (26) Harvey, O. R.; Kuo, L. J.; Zimmerman, A. R.; Louchouart, P.; Amonette, J. E.; Herbert, B. E. An Index-Based Approach to Assessing Recalcitrance and Soil Carbon Sequestration Potential of Engineered Black Carbons (Biochars). *Environ. Sci. Technol.* **2012**, *46*, 1415-1421.
- (27) Li, F.; Cao, X.; Zhao, L.; Wang, J.; Ding, Z. Effects of Mineral Additives on Biochar Formation: Carbon Retention, Stability, and Properties. *Environ. Sci. Technol.* **2014**, *48*, 11211-11217.
- (28) Burhenne, L.; Messmer, J.; Aicher, T.; Laborie, M. P. The effect of the biomass components lignin, cellulose and hemicellulose on TGA and fixed bed pyrolysis. *J. Anal. Appl. Pyrolysis* **2013**, *101*, 177-184.
- (29) Raveendran, K.; Ganesh, A.; Khilar, K. C. Influence of mineral matter on biomass pyrolysis characteristics. *Fuel* **1995**, *74*, 1812-1822.
- (30) Zhao, L.; Zheng, W.; Cao, X.D. Distribution and evolution of organic matter phases during biochar formation and their importance in carbon loss and pore structure. *Chem. Eng. J.* **2014**, *250*, 240-247.
- (31) Chen, B.; Zhou, D.; Zhu, L. Transitional adsorption and partition of nonpolar and polar aromatic contaminants by biochars of pine needles with different pyrolytic temperatures. *Environ. Sci. Technol.* **2008**, *42*, 5137.
- (32) Patwardhan, P. R.; Satrio, J. A.; Brown, R. C.; Shanks, B. H. Influence of inorganic salts on the primary pyrolysis products of cellulose. *Bioresour. Technol.* **2010**, *101*, 4646.
- (33) He, M.; Hu, Z.; Xiao, B.; Li, J.; Guo, X.; Luo, S.; Yang, F.; Feng, Y.; Yang, G.; Liu, S. Hydrogen-rich gas from catalytic steam gasification of municipal solid waste (MSW): Influence of catalyst and temperature on yield and product composition. *Int. J. Hydrogen Energy* **2009**, *34*, 195-203.
- (34) Leng, E.; Wang, Y.; Gong, X.; Zhang, B.; Zhang, Y.; Xu, M. Effect of KCl and CaCl<sub>2</sub> loading on the formation of reaction intermediates during cellulose fast pyrolysis. *Proc. Combust. Inst.* **2017**, *36*, 2263-2270.
- (35) Ateş, F.; Pütün, A. E.; Pütün, E. Fixed bed pyrolysis of Euphorbia rigida with different catalysts. *Energy Convers. Manage.* **2005**, *46*, 421-432.
- (36) Spokas, K. A.; Novak, J. M.; Masiello, C. A.; Johnson, M. G.; Colosky, E. C.; Ippolito, J. A.; Trigo, C. Physical Disintegration of Biochar: An Overlooked Process. *Environ. Sci. Technol. Lett.* **2014**, *1*, 326-332.

- (37) Xiao, X.; Chen, B.; Zhu, L. Transformation, Morphology, and Dissolution of Silicon and Carbon in Rice Straw-Derived Biochars under Different Pyrolytic Temperatures. *Environ. Sci. Technol.* **2014**, *48*, 3411-3419.
- (38) Chen, Z.; Chen, B.; Chiou, C. T. Fast and slow rates of naphthalene sorption to biochars produced at different temperatures. *Environ. Sci. Technol.* **2012**, *46*, 11104-11111.
- (39) Bustin, R. M.; Guo, Y. Abrupt changes (jumps) in reflectance values and chemical compositions of artificial charcoals and inertinite in coals. *Int. J. Coal Geol.* **1999**, *38*, 237-260.
- (40) Chua, Y. W.; Yu, Y.; Wu, H. Thermal decomposition of pyrolytic lignin under inert conditions at low temperatures. *Fuel* **2017**, *200*, 70-75.
- (41) Chen, Z.; Xiao, X.; Chen, B.; Zhu, L. Quantification of Chemical States, Dissociation Constants and Contents of Oxygen-containing Groups on the Surface of Biochars Produced at Different Temperatures. *Environ. Sci. Technol.* **2015**, *49*, 309.
- (42) Qian, L.; Chen, B. Dual Role of Biochars as Adsorbents for Aluminum: The Effects of Oxygen-Containing Organic Components and the Scattering of Silicate Particles. *Environ. Sci. Technol.* **2013**, *47*, 8759-8768.
- (43) Tian, K.; Liu, W. J.; Qian, T. T.; Jiang, H.; Yu, H. Q. Investigation on the evolution of N-containing organic compounds during pyrolysis of sewage sludge. *Environ. Sci. Technol.* **2014**, *48*, 10888.
- (44) Baker, M. A.; Hammer, P. A Study of the Chemical Bonding and Microstructure of Ion Beam-deposited CN<sub>x</sub> Films Including an XPS C 1s Peak Simulation. *Surf. Interface Anal.* **2015**, *25*, 629-642.
- (45) Yuan, S.; Gu, J.; Zheng, Y.; Jiang, W.; Liang, B.; Pehkonen, S. Purification of phenol-contaminated water by adsorption with quaternized poly(dimethylaminopropyl methacrylamide)-grafted PVBC microspheres. *J. Mater. Chem. A* **2015**, *3*, 4620-4636.
- (46) Joseph, S. D.; Campsarbertain, M.; Lin, Y.; Munroe, P.; Chia, C. H.; Hook, J.; Zwieten, L. V.; Kimber, S.; Cowie, A.; Singh, B. P. An investigation into the reactions of biochar in soil. *Aust. J. Soil Res.* **2010**, *48*, 501-515.
- (47) Qian, T. T.; Li, D. C.; Jiang, H. Thermochemical Behavior of Tris(2-Butoxyethyl) Phosphate (TBEP) during Co-pyrolysis with Biomass. *Environ. Sci. Technol.* **2014**, *48*, 10734-10742.
- (48) Liu, X. Q.; Ding, H. S.; Wang, Y. Y.; Liu, W. J.; Jiang, H. Pyrolytic Temperature Dependent and Ash Catalyzed Formation of Sludge Char with Ultra-High Adsorption to 1-Naphthol. *Environ. Sci. Technol.* **2016**, *50*, 2602-2609.
- (49) Yang, Y.; Shu, L.; Wang, X.; Xing, B.; Tao, S. Impact of De-Ashing Humic Acid and Humin on Organic Matter Structural Properties and Sorption Mechanisms of Phenanthrene. *Environ. Sci. Technol.* **2011**, *45*, 3996-4002.
- (50) Smith, M. W.; Dallmeyer, I.; Johnson, T. J.; Brauer, C. S.; Mcewen, J. S.; Espinal, J. F.; Garcia-Perez, M. Structural analysis of char by Raman spectroscopy: Improving band assignments through computational calculations from first principles. *Carbon* **2016**, *100*, 678-692.
- (51) Guizani, C.; Haddad, K.; Limousy, L.; Jeguirim, M. New insights on the structural evolution of biomass char upon pyrolysis as revealed by the Raman spectroscopy and elemental analysis. *Carbon* **2017**, *119*, 519-521.
- (52) Nielsen, H. P.; Baxter, L. L.; Schluppab, G.; Morey, C.; Frandsen, F. J.; Dam-Johansen, K. Deposition of potassium salts on heat transfer surfaces in straw-fired boilers: a pilot-scale study. *Fuel* **1999**, *79*, 131-139.
- (53) Chen, Z.; Chen, B.; Zhou, D.; Chen, W. Bisolute sorption and thermodynamic behavior of organic

pollutants to biomass-derived biochars at two pyrolytic temperatures. *Environ. Sci. Technol.* **2012**, *46*, 12476-12483.

(54) Liu, W. J.; Li, W. W.; Jiang, H.; Yu, H. Q. Fates of Chemical Elements in Biomass during Its Pyrolysis. *Chem. Rev.* **2017**, *117*, 6367–6398.

(55) Torsten Kowalski, †; Christian Ludwig, †, ‡ And; Wokaun†, A. Qualitative Evaluation of Alkali Release during the Pyrolysis of Biomass. *Energy Fuels* **2007**, *21*, 3017-3022.

(56) Hu, S.; Jiang, L.; Wang, Y.; Su, S.; Sun, L.; Xu, B.; He, L.; Xiang, J., Effects of inherent alkali and alkaline earth metallic species on biomass pyrolysis at different temperatures. *Bioresour. Technol.* **2015**, *192*, 23-30.

Table 1. Elemental components and inherent minerals removal of the biomasses

Elements	C	H	N	S	K	Ca	Mg	Fe	Al	Ash	Minerals removal rate
	%										
BG	39.9	5.86	0.84	0.43	2.28	2.56	0.229	0.081	0.031	<b>8.62</b>	<b>88.7</b>
DM-BG	46.6	6.16	0.58	0.10	0.03	0.53	0.068	0.024	0.131	0.97	/
PH	44.1	5.95	1.20	0.24	1.77	1.50	0.183	0.165	0.175	<b>4.64</b>	<b>81.7</b>
DM-PH	48.4	5.98	0.73	0.07	0.02	0.32	0.037	0.139	0.055	0.85	/
CM	37.9	5.63	1.88	0.39	2.43	1.43	0.274	0.204	0.093	<b>15.1</b>	<b>85.3</b>
DM-CM	47.5	6.10	2.07	0.26	0.11	0.58	0.028	0.066	0.025	2.22	/
SS	34.8	5.10	4.04	0.94	0.96	1.24	0.177	2.747	0.96	<b>35.6</b>	<b>51.5</b>
DM-SS	42.6	6.02	5.19	1.07	0.51	0.37	0.034	0.558	0.243	17.3	/

(BG: barley grass; DM-BG: demineralized barley grass; PH: peanut hull; DM-PH: demineralized peanut hull; CM: cow manure; DM-CM: demineralized cow manure; SS: sewage sludge; DM-SS: demineralized sewage sludge)

Table 2. Percent of the peak area determined by XPS

Biochar	C-C/C=C	C-O	C=O	O=C-O
CM	63.6	25.5	5.68	5.18
DM-CM	76.1	18.0	3.44	2.46

(CM: cow manure; DM-CM: demineralized cow manure)

Table 3. Raman structural parameters of different biochars

Biochar	$I_G/I_{All}$	$I_D/I_G$
BG	0.54	1.23
DM-BG	0.66	1.07
PH	0.57	1.18
DM-PH	0.62	1.11
CM	0.51	1.34
DM-CM	0.72	1.13
SS	0.55	1.22
DM-SS	0.62	1.16

(BG: barley grass; DM-BG: demineralized barley grass; PH: peanut hull; DM-PH: demineralized peanut hull; CM: cow manure; DM-CM: demineralized cow manure; SS: sewage sludge; DM-SS: demineralized sewage sludge)



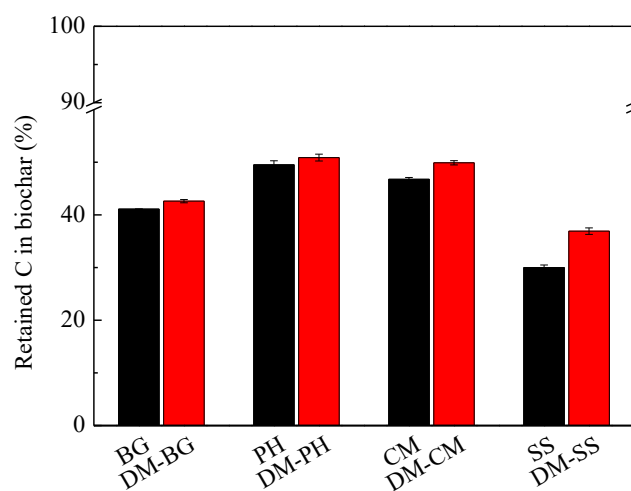


Figure 1. Carbon retained in the biochars derived from different biomasses with or without inherent minerals. (BG: barley grass; DM-BG: demineralized barley grass; PH: peanut hull; DM-PH: demineralized peanut hull; CM: cow manure; DM-CM: demineralized cow manure; SS: sewage sludge; DM-SS: demineralized sewage sludge)

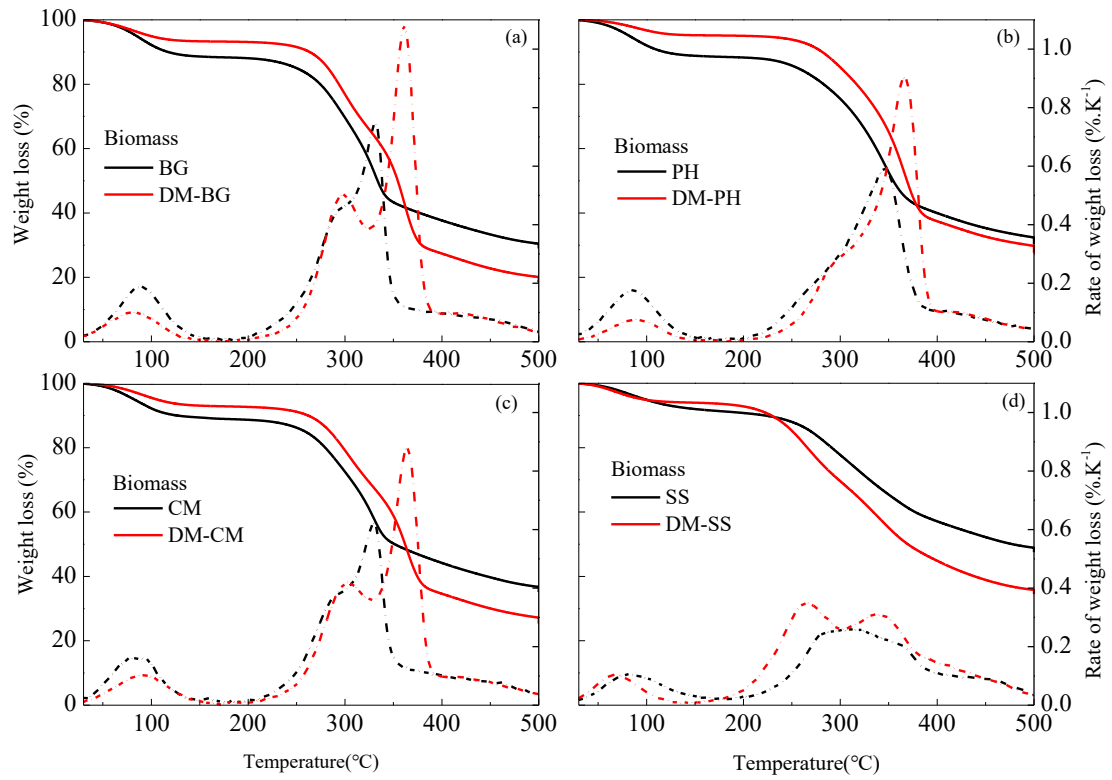


Figure 2. TGA and DTG curves of the biomasses under  $N_2$  atmosphere to simulate the pyrolysis process. (BG: barley grass; DM-BG: demineralized barley grass; PH: peanut hull; DM-PH: demineralized peanut hull; CM: cow manure; DM-CM: demineralized cow manure; SS: sewage sludge; DM-SS: demineralized sewage sludge)

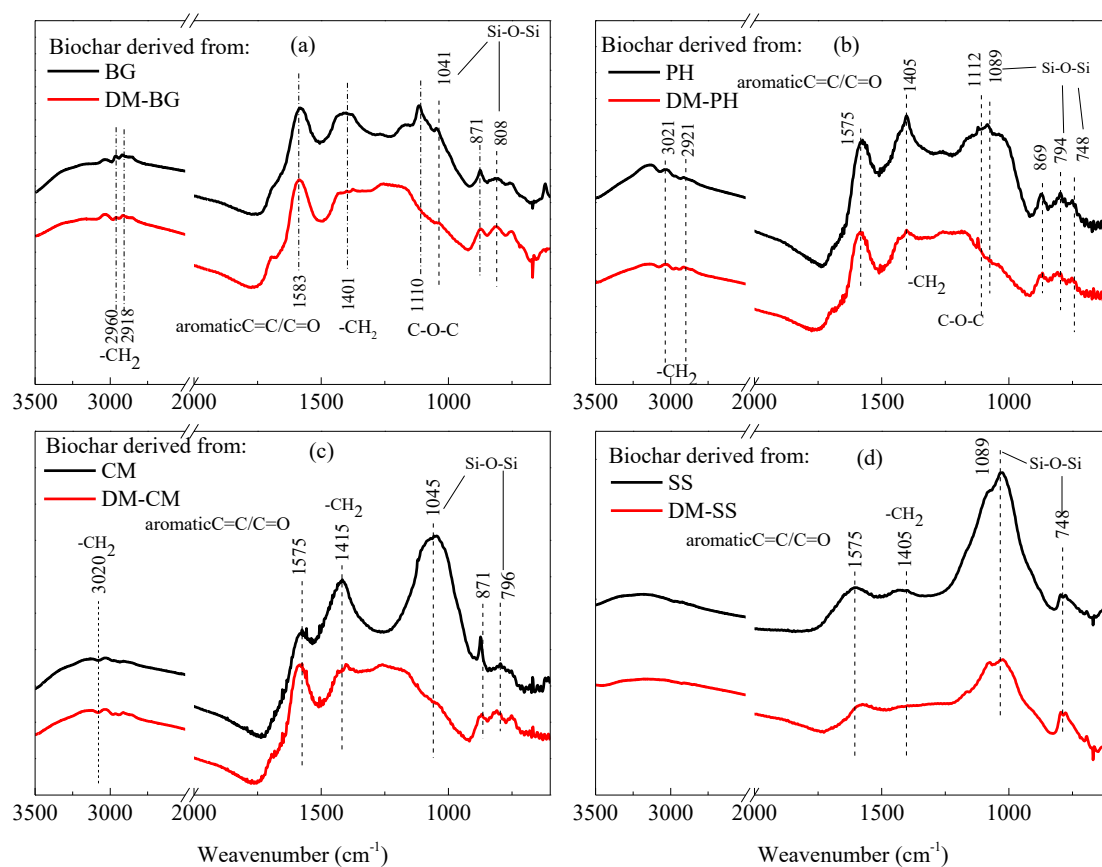


Figure 3. FTIR spectra of the biochars derived from the demineralized and pristine biomasses.

(BG: barley grass; DM-BG: demineralized barley grass; PH: peanut hull; DM-PH: demineralized peanut hull; CM: cow manure; DM-CM: demineralized cow manure; SS: sewage sludge; DM-SS: demineralized sewage sludge)

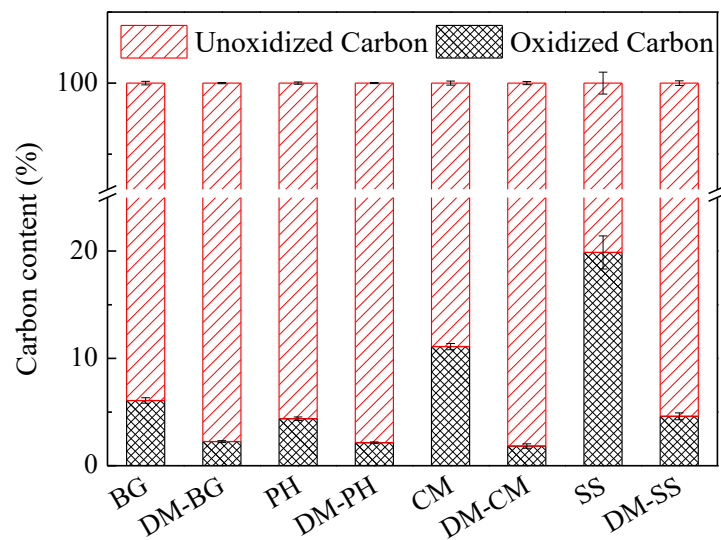


Figure 4. Carbon loss rate of the biochars after  $K_2Cr_2O_7$  oxidation. (BG: barley grass; DM-BG: demineralized barley grass; PH: peanut hull; DM-PH: demineralized peanut hull; CM: cow manure; DM-CM: demineralized cow manure; SS: sewage sludge; DM-SS: demineralized sewage sludge)

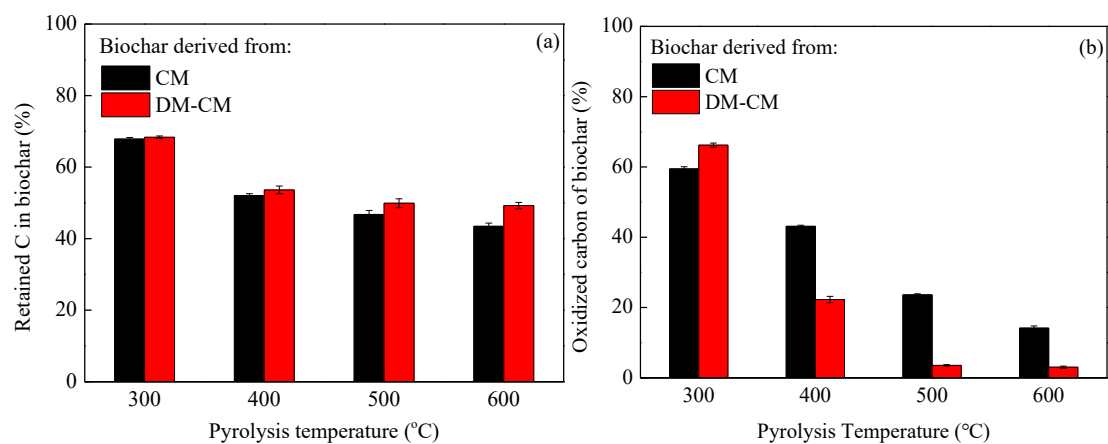


Figure 5. Under 300-600°C carbon retention (a) and the oxidation resistance (b) of the biochars (take cow manure (CM) and the demineralized cow manure (DM-CM) as the representative example)

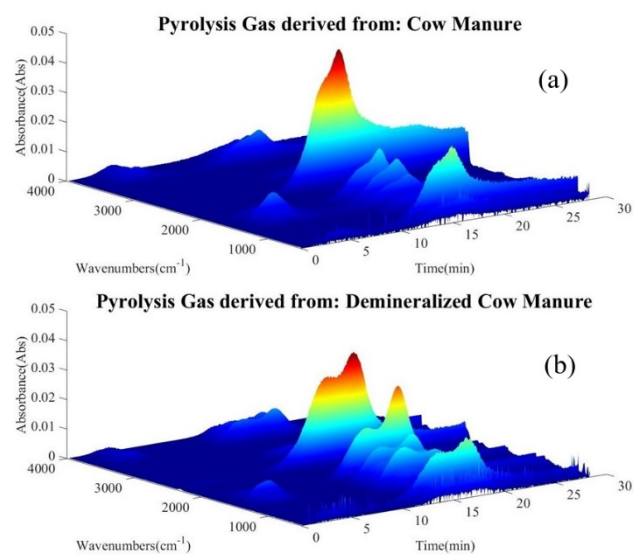
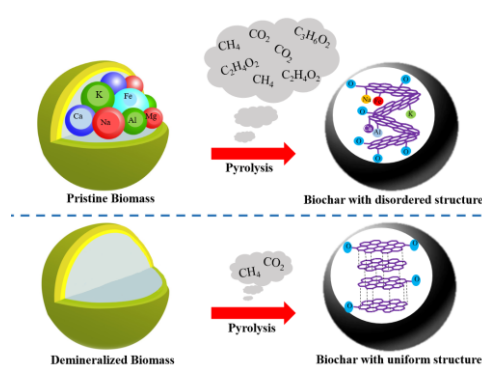


Figure 6. TG-FTIR curves of the pyrolysis gas for the original (a) and demineralized (b) cow manure (CM and DM-CM).

## Graphic abstract



**Synopsis:** An environmentally friendly carbon sequestration approach was established through removing the inherent minerals to change the pyrolysis process of biomass.